

Trends in Dispersion Coatings in Japan

Tadao Hayashi, Osaka Prefecture University, Osaka, Japan.

Main topics in dispersion coatings in the past decade have been the reparation of wear resistant coatings. Recently, new application was focused on the various types of coating systems in order to develop new materials in many fields, such as photosensitive metal coatings, solar cell type films, Pb-free solder plating, and etc. The aim of this paper is to review some of the new research and developments in dispersion coatings (composite coatings) in Japan, based on the papers published in the technical journals in the past five years.

For more information, please contact:

Dr. Tadao Hayashi (Osaka Prefecture University)

Home address:

4-17-17, Tezukayama-Minami

Nara-shi, 631-0064, Japan

TEL & FAX: +81-742-47-1938

E-mail: drhayasi@ca.mbn.or.jp

Main topics in dispersion coatings in the past decade have been the preparation of wear resistant coatings. Recently, new application was focused on the various types of coating systems in order to develop new materials in many fields, such as photosensitive metal coatings, solar cell type films, Pb-free solder plating, and etc. The aim of this paper is to review some of the new research and developments in dispersion coatings (composite coatings) in Japan, based on the papers published in the technical journals in the past five years. The following dispersion coating systems have been studied in the past in Japan. Ni-Al₂O₃, Ni-TiO₂, Ni-fluorescence pigment, Ni/Co-SiC, Ni/Mn/S-SiC, Ni/Co-Si₃N₄, Ni/P-CaF₂, Ni/Co/P-BN, Zn-Al₂O₃, Ni-Diamond, Ag-La₂O₃, Cu-ZrB₂, Ag-ZrB₂, Zn-SiO₂, Ni-SiO₂, Zn/Co-SiO₂, Pt-PTFE, Ag-PTFE, Cu-TiO₂, Zn-TiO₂. Dispersion coatings studied at the Osaka Prefecture University are shown in Table 1.

Table 1. Dispersion coatings studied at Osaka Prefecture University

- 1) Electrodeposition of Ni-Al₂O₃, Ni-TiO₂ and Ni-ZrO₂ dispersion coatings (1976)
- 2) Preparation of Ni-Al₂O₃ and Ni-ZrO₂ dispersion coatings (1977)
- 3) Colored Ni plating using fluorescent pigment (1980)
- 4) Electrodeposition of Ni-B₄C dispersion coatings (1982)
- 5) Ni-Mn-S-SiC dispersion hardening alloy coatings (1983)
- 6) Electrodeposition of Ni-Co-SiC dispersion coatings (1984)
- 7) Electrodeposition of Zn dispersion coatings (1987)
- 8) Electroplating of a new colored dispersion coatings (1988)
- 9) Preparation of Ni-B-SiC composite coatings by electroless plating (1989)
- 10) Electrodeposition and some properties of Ni-Co-Si₃N₄ dispersion coatings (1990)
- 11) On the electrodeposition of new colored dispersion coatings (1990)
- 12) Electrodeposition and properties of Ni-P-CaF₂ dispersion coatings (1992)
- 13) Electrodeposition and characterization of Ni-Co-BN dispersion coatings (1995)

New type of dispersion coatings

1) Non-aqueous electrolyte in dispersion coatings

Hirato¹⁾ tried to deposit Al composite plating containing nanometer-sized particles from a non-aqueous electrolyte. Electrolyte used was prepared by mixing 150 g dimethylsulfone (DMSO₂) with 42.2 g AlCl₃ and the appropriate amount of particles in a glass plating cell provided with a sealed glove box. Dispersoids used in this study were 200 nm SiO₂ and 50 nm Al₂O₃. In their previous study, they found that the decreasing hydrophilicity of the particles is an effective way to enhance the codeposition of particles from aqueous

electrolyte.²⁾

Therefore, they tried to use a non-aqueous electrolyte in order to enhance the codeposition of strongly hydrophilic particles like SiO₂ and Al₂O₃. Fig. 1 shows the SEM picture of the surface morphology of as-plated composite Al-SiO₂ deposit electroplated from the AlCl₃-DMSO₂ bath containing 30 g/dm³ SiO₂ at a current density of 13 A/dm². In this picture, codeposition of spherical SiO₂ particles was observed into Al matrices. No agglomeration of the particles was found in this Al-SiO₂ dispersion coatings.

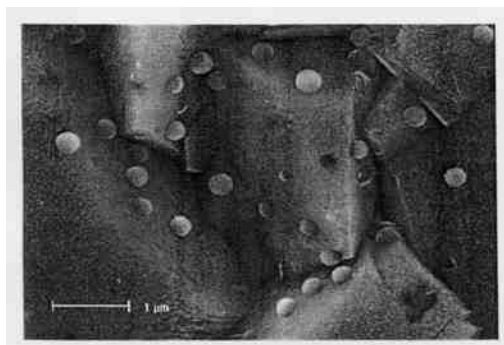


Fig. 1 SEM micrograph of Al-SiO₂ composite coating obtained from AlCl₃-DMSO₂ bath

Cross section of the Al-SiO₂ deposit obtained from the same bath containing 53 g/dm³ SiO₂ at a current density of 8 A/dm² is shown in Fig. 2.

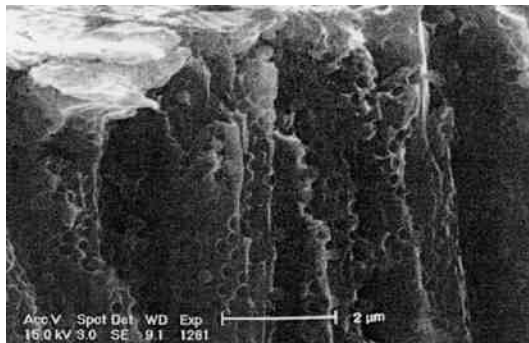


Fig. 2 SEM micrograph of the cross section of Al-SiO₂ deposit

Homogeneous distribution of the SiO₂ particles was found in the cross section of the film. The SiO₂ content in the Al matrix was found to be 2 vol.% when SiO₂ concentration was 2 g/dm³, and 12 vol.% in the case of SiO₂ 20 g/dm³. The large amount of codeposition of hydrophilic particles (SiO₂ and Al₂O₃) confirms that the elimination of the hydration force achieved by using non-aqueous electrolytes significantly enhance the codeposition of such particles and can avoid the agglomeration which takes place in aqueous electrolyte. This process opens the new fields of application for the preparation of dispersion coatings containing homogeneously dispersed nanometer-sized particles.

DMSO₂ may be used as a solvent for the non-aqueous metal compounds other than Al₂O₃. The formation of Al alloy and also other various metals can be applied for the preparation of composite coatings. They also tried to deposit Al-TiO₂ dispersion coatings using AlCl₃-DMSO₂ bath.

Dispersoids used in this study were TiO₂(10 nm particle size) and carbon nanotube(CNT).³⁾ Electrodeposition was carried out at 110°C by means of galvanostatic method with the total current of 120 C/cm². The TiO₂ content in Al-TiO₂ dispersion coating was found to be 40 vol.% compared to 10vol.% in Ni-TiO₂ coating obtained from an aqueous solution.

In the mapping of Ti element in the Al-TiO₂ coating, the homogeneous dispersed TiO₂ was found in the dispersion coating. On the other hand, agglomeration of the TiO₂ particles was observed in the Ni-TiO₂ coatings. Moreover, the codeposition of CNT was confirmed in the Al-CNT dispersion coatings obtained from AlCl₃-DMSO₂ bath containing 5 g/l CNT with a current density of 80 mA/cm². These results imply that the electrodeposition of nano-sized dispersion coatings from non-aqueous electrolyte seemed to be the unique preparation of new type of dispersion coatings homogeneously dispersed nano-metersized particles.

2) Composite photosensitive electrode prepared by dispersion plating

Ise et al.⁴⁾ tried to prepare Ni-AgBr composite photosensitive electrode by dispersion plating. Photosensitive composite electrode for an electrolytic cell aimed at energy conversion and photoredox reactions was prepared by the dispersion coating. Watts Ni plating bath was used for the dispersion coatings. Composition of the Watts bath is given below;

NiSO ₄ • 6H ₂ O	300 g/dm ³
NiCl ₂ • 6H ₂ O	45 g/dm ³
H ₃ BO ₃	30 g/dm ³

AgBr particles were added to the 100 ml Watts bath to get the dispersion coatings.

The effect of pH of the bath on AgBr content in Ni-AgBr coating was shown in Fig. 3.

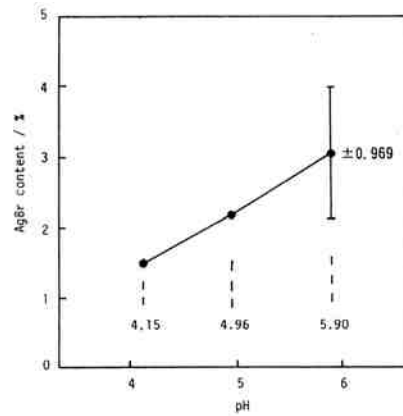


Fig. 3 AgBr content in Ni-AgBr composite coating vs. pH of the bath
(Temp. 70°C, 900 rpm, current density 5 A/dm², plating time 45 min. 4500°C)

To get a photosensitive Ni-AgBr composite electrode containing large amount of AgBr, deposition condition was carefully controlled by adjusting pH of the bath, current density and the stirring of the electrolyte. The pH of the bath was found to be best at 5.9. The lower current density seemed to be preferable to get a large amount of AgBr in the Ni matrices. The SEM photograph of the Ni-AgBr dispersion coating is shown in Fig. 4. The cationic surfactant generally improves the codeposition of AgBr into Ni-matrices owing to the surface charge of the AgBr particles. The Ni-AgBr electrode prepared by the dispersion plating resulted in the transformation of light energy to the electric energy.

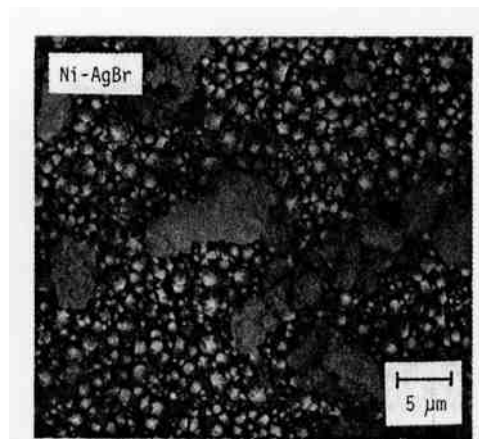


Fig. 4 SEM micrograph of Ni-AgBr dispersion coating

These results can be evaluated by the cyclic voltammogram obtained with or without the radiation of light to the electrode in 0.1 M NaOH which is shown in Fig. 5.

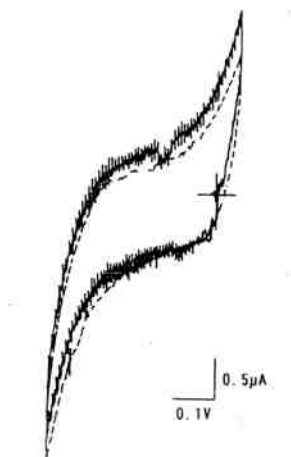


Fig. 5 Cyclic voltammogram of Ni-AgBr electrode in 0.1 M NaOH
(Scan rate 10 mV/s. Pot. V vs. Ag/AgCl, Dark: ••••, Chopped: ----)

Furthermore, these types of the electrode can be used as a photosensitive electrode for the photoredox reactions.

3) Photocatalytic activity of Ag-TiO₂ dispersion coatings

Yamaguchi et al.⁵⁾ prepared Ag-TiO₂ dispersion coatings and evaluated their photocatalytic activity. Ag-TiO₂ and Cu-TiO₂ dispersion coatings have been tested for the photocatalytic activity in Brilliant Green(B.G.) solution to measure the decomposition rate. Measurement of the photocatalytic activity of the Ag-TiO₂ coating was carried out in the following way; The test electrode, Ag-TiO₂ was dipped in 5 ml of 10 ppm B. G. solution. UV light was radiated to the electrode under the constant time, then the concentration of B.G. was measured by the absorption method.(UV mini 1240, Shimazu) Decomposition rate of B.G. was estimated by the absorption curve.

Fig. 6 shows the effect of quantity of electricity on the codeposited TiO₂.

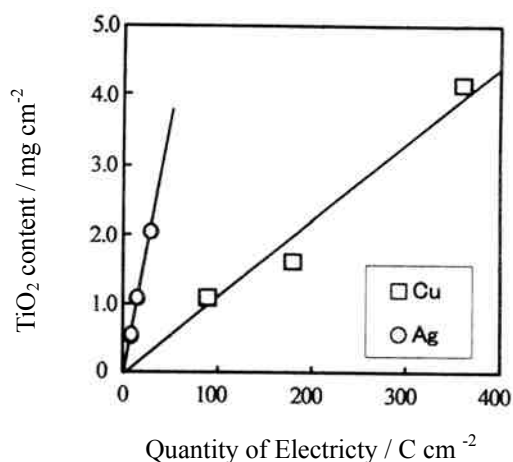


Fig. 6 Effect of current on the codeposition of TiO₂ in Ag and Cu films

Fig. 7 shows the photocatalytic activity of Ag-TiO₂ and Cu-TiO₂.

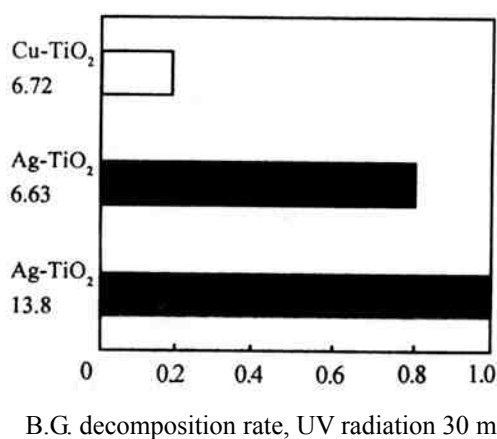


Fig. 7 Photocatalytic activity of Ag-TiO₂ and Cu-TiO₂ electrodes

It was found that the formation of oxygen on the Ag electrode seemed to be greater compared to the Cu electrode which reflected the higher rate of oxidative decomposition of B.G...

4) Water repellent Metal/Ni-PTFE composite films

Ibe et al.⁶⁾ prepared the water repellent Metal/Ni-PTFE composite films and tested their properties on the corrosion resistance. To improve the corrosion resistance of Ni-PTFE composite film, electrodeposition of Au, Cr, Sn on the composite coatings to form Metal/Ni-PTFE double layered composite film has been studied. The contact angles of the water drop on Ni-PTFE and also Metal/Ni-PTFE composite films (Metal, Au, Cr, Sn) were found to be 155, 153, 145 and 151, respectively. Cr/Ni-PTFE composite film has the smallest corrosion current among the metal/Ni-PTFE composite coatings studied. The amount of Ni dissolved from the samples

increased in the order of Ni-PTFE, Sn/Ni-PTFE, Cr/Ni-PTFE and Au/Ni-PTFE. The change in the wettability of the samples seemed to affect the corrosion behavior of the composite coatings. The double layered composite coatings have been prepared by the following methods.

Substrate: Polished Ni plate(99.7% purity, 50 mmx70mmx0.1 mm) Ni plate was plated with Wood Ni strike(0.5 μ m) followed by Watts Ni plating(2.0 μ m). Ni-PTFE composite coatings were prepared by using a Ni sulfamate bath at 50°C. Thickness of the deposits was 10 μ m. PTFE powder was a product of Central glass Ltd.(polymerized degree, 8.0×10^2 - 1.0×10^4 , mean particle size 5 μ m). PTFE particle was added to the 0.1% cationic surfactant solution(1:1) and agitated strongly with homogenizer, then introduced to the Ni sulfamate bath. Ni-PTFE composite plating thus prepared were washed with water and Au, Cr, and Sb were plated on the Ni-PTFE composite coating from each plating bath. Au plated from alkaline cyanide bath, Cr from Sargent bath, and Sn from alkanol sulfonate bath, respectively. In each plating, the thickness of the metal deposit was controlled to be 0.1 μ m. Table 2 shows the plating bath constitutions and plating conditions. The composition of the composite coatings were analyzed by fluorescent X-ray analyzer(SXF-1100S, Shimazu). The contact angle of the water drop on the coatings were measured by contact angle analyzer(CA-X, Kyowa Kaimen Kagaku). Surface morphology of the composite coatings were measured by SEM(JSM-5800LV, Nihon denshi), Microanalyzer (JXA-8900L) and ESCA (5500MC/SAM, PHI). Electric resistance of the coating film was measured by LCR meter (H.P.LCR meter 4261A, Yokogawa). Electrochemical measurement of the deposited composite coatings were carried out by using a potentiostat/galvanostat (EG&G 283). In the dipping test of the samples in 1 mol/dm³ HCl at 25°C, corrosion loss of the coatings was measured in every 6hr in the course of test.

Table 2 Bath composition and plating conditions

Plating bath	Reagent	Conditions			
		C	T	I	t
Ni strike (Wood's bath)	NiCl ₂ 6 H ₂ O	: 1.20	R.T.	6	120
	HCl	: 2.50			
Ni undercoat (Watts bath)	NiSO ₄ 6 H ₂ O	: 0.86	50	3	300
	NiCl ₂ 6 H ₂ O	: 0.19			
	HBO ₃	: 0.43			
Ni-PTFE/Ni composite	(NH ₂ SO ₃) ₂ 4 H ₂ O	: 1.40	50	3	1200
	NiCl ₂ 6 H ₂ O	: 0.06			
	HBO ₃	: 0.43			
	PTFE(0~0.35 kg dm ⁻³)				
Au plating	KAu(CN) ₂ H ₂ O	: 0.03	60	3	10
	KCN	: 1.23			
Cr plating	CrO ₃	: 2.00	60	25	60
	H ₂ SO ₄	: 0.02			
Sn plating	Sn ²⁺	: 0.30	20	2	20
	H ₂ SO ₄	: 0.02			

Fig. 8 shows the contact angle of a water drop on the surface of the Metal/Ni-PTFE composite films heat-treated at 300°C, 325°C and 350°C.

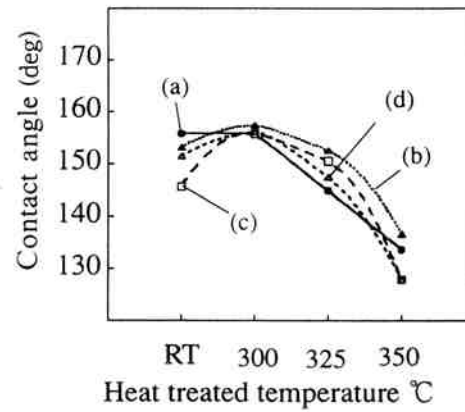


Fig. 8 Contact angle of a water drop on the surface of the Metal/Ni-PTFE composite films heat-treated
 (a) Ni (b) Ni-PTFE (c) Au/Ni-PTFE (d) Cr/Ni-PTFE

Table 3 shows the electric resistance of the surface of various coating systems.

Table 3 Electric resistance on the surface of various materials

Materials	Electric resistance($\times 10^{-4} \Omega \text{m}^{-1}$)
Ni	5.41
Ni-PTFE	14.40
Au/Ni-PTFE	5.26
Cr/Ni-PTFE	3610.00
Sn/Ni-PTFE	9.33

The corrosion behavior of the composite coatings was shown in Fig. 9.

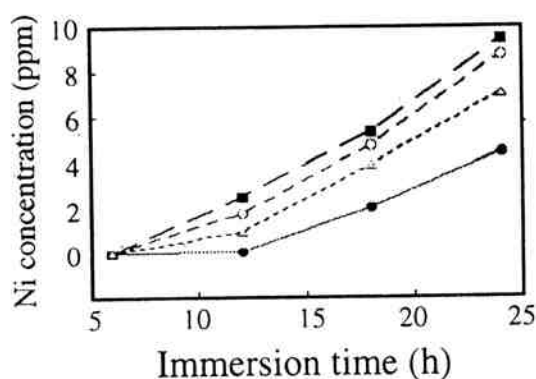


Fig. 9 Corrosion test of Metal/Ni-PTFE composite films in 1 M HCl solution.

(● Ni-PTFE; ■ Au/Ni-PTFE; ○ Cr/Ni-PTFE; Δ Sn/Ni-PTFE)

Metal/Ni-PTFE double layered composite coatings gave the fairly good water repellent properties with the contact angle of water over 145° , when they were heat-treated at 325°C . In the electrochemical corrosion test in HCl solution, Cr/Ni-PTFE composite film was found to have the smallest corrosion current among the various composite films studied.

In the immersion test of the samples in 1 M HCl solution, no dissolution of Ni was observed before 6hr in the course of corrosion test.

5) Ni-ceramic particles composite coatings from ethanol bath.

Saji et al.⁷⁾ tried to investigate the co-deposition of various ceramic particles with Ni using an ethanol bath and to study the wear resistance of these coatings.

A new type of bath containing $200 \text{ g/dm}^3 \text{ NiCl}_2 \cdot 6\text{H}_2\text{O}$ and $9 \text{ ml/dm}^3 \text{ HCl}(35-37\%)$ in EtOH(99.5%) was used for the composite plating. 10 g/dm^3 ceramic particles were added to the above bath and the ultrasonically agitated for 5 min. followed by the stirring for 5 min. just before plating.

Ceramic particles used in this study were WC, Al_2O_3 , SiC, BC and Diamond. The amount of incorporated particles into Ni matrices was measured gravimetrically and morphology of the coatings was evaluated by using SEM.

The wear resistance of the coatings was examined by the abrasion tester fitted with a SiC ($10\mu\text{m}$) counter surface under the load of 2.5 kg for 300 cycles at a dry sliding condition with the room temperature in air.

A typical SEM image of the cross section of the Ni- Al_2O_3 composite coating obtained from the ethanol bath is shown in Fig. 10.

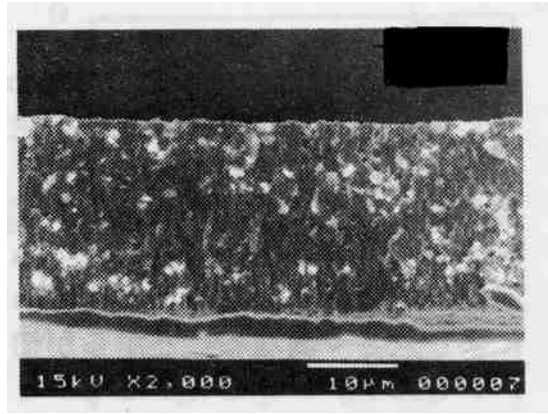


Fig. 10 SEM image of a cross section of the Ni-Al₂O₃ composite coating from the ethanol bath.

The wear resistance of the various composite coatings were shown in Fig. 11.

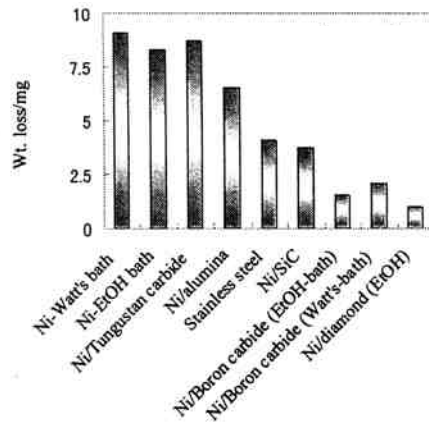


Fig. 11 Wear resistance of the various composite coatings.

The wear resistance of the composite coatings using the ethanol bath exhibited the better anti-wear performance than that of the coatings obtained from an aqueous Ni bath. The better wear resistance of the new composite coatings might be due to the nickel matrices with finely dispersed ceramic particles codeposited from the ethanol bath.

6) Sn-Ag composite coatings

Fujiwara et al.⁸⁾ developed the unique process in the preparation of Sn-Ag alloy deposit by the composite plating. Electrolyte was prepared by an addition of concentrated AgNO₃ solution into SnSO₂-K₄P₂O₇ electrolyte and PEG #6000 was added to the bath. Upon mixing the both solution, the electrolyte turned heavy black-brown color and the superfine Ag particle was formed in the solution. In the plating bath, Sn exists as the uncomplexed form as SnP₂O₇²⁻ and Ag as a very fine powder with its average particle size of 2.4-5.0 nm. In the pH range 7-9, Ag

content in the Sn-Ag alloy deposit was found to be about 3wt.% and this composition is the same that of eutectic Sn-Ag alloy. The Sn-Ag alloy deposit obtained in this process was found to give the equilibrium phase structure with β -Sn and Ag_3Sn which melted at eutectic temperature(221°C) of the Sn-Ag alloy. Solderability of the composite plated Sn-Ag alloy evaluated by the zero-cross time seemed to be fairly good and there is no defect in the humidity test.

7) Composite plating of Ni/SiC using a cationic surfactant with an azobenzene group.

Saji et al.⁹⁾ studied the composite plating of Ni-SiC using a cationic surfactant containing an azobenzene group(AZTAB) which enable to increase the content of SiC particle in the composite. Molecular structure of AZTAB is shown in Fig. 12.

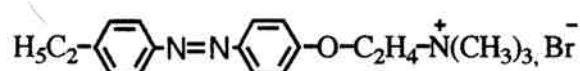


Fig. 12 Molecular structure of AZTAB

The composition and operating conditions of the bath are shown in Table 4.

The α -type SiC particles labeled as 1 μm particle size (Soekawa Chemicals, Japan) were used without purification. The substrate was a copper plate and a Ni plate was used as an anode. The morphology of the surface and cross section of the coatings were examined using a SEM and the amount of the codeposits and SiC was determined by using an energy disperse X-ray(EDX) microanalyzer coupled to the SEM at a magnification of 100 times and an accelerating voltage of 15 kV.

Table 4 Bath composition and operating conditions

NiSO ₄ ·6H ₂ O	300 g dm ⁻³
NiCl ₂ ·6H ₂ O	60 g dm ⁻³
H ₃ BO ₃	40 g dm ⁻³
Electrolyte volume	50 mL
AZTAB	0 ~ 5 g dm ⁻³
SiC	2 ~ 100 g dm ⁻³
pH	1 (with HCl)
Magnetic stirrer	2 cm long, 7 mm diam bar, about 300 rpm
Temperature	30 ~ 70°C
Current density	2 ~ 20 A dm ⁻²

The ZHF corrected EDX data were used to determine the atomic percentage of Ni and Si from the intensity of the respective K _{α} lines. The volume percentage of Si calculated is represented as the total content of SiC in the coatings. The variables of the bath (Table 4) for maximum codeposition of SiC was optimized under the following conditions: 3.5 g/dm³ AZTAB, 15 g/dm³ SiC, 10 A/dm² and 50°C. Under these conditions, the content of SiC in the deposits was found to be 62.4±0.8 vol.%, and the volume % of SiC measured at 3 different locations of the same coating layer within a range of ±0.3%.

Fig. 13 shows the effect of the surfactant concentration on the extent of the SiC codeposition.

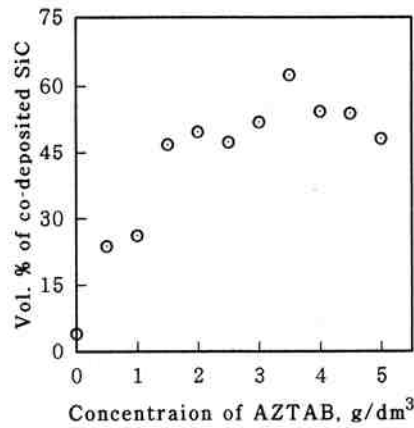


Fig. 13 Effect of concentration of AZTAB on the extent of codeposition of SiC
(SiC 15g/dm³, 10 A/dm², 50°C)

The increase in the codeposition of SiC into Ni matrix might be due to the strong adsorption of AZTAB on SiC particles which probably charges the surface of the particles more positively and hence increases the affinity of the particles for the negatively charged cathode. As the results, the higher rate of codeposition even with a much lower particle concentration in the bath was achieved.

The SEM photographs of the dispersion coatings are shown in Fig. 14.

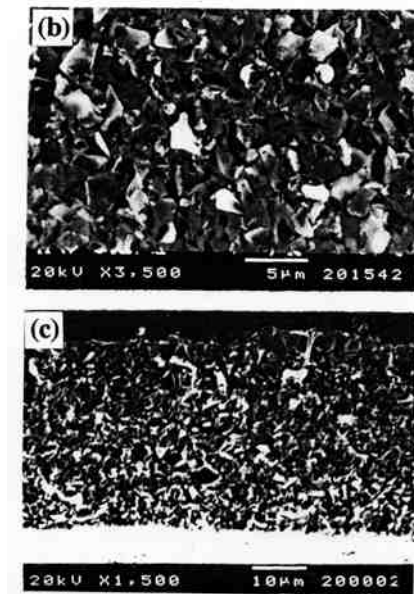


Fig. 14 SEM micrographs of the surface(b) and cross section(c)
of the Ni-SiC composite coating on Cu plate

The surface of the Ni-SiC composite prepared under the optimum conditions was uniform and smooth. The surface morphology of this composite shows the uniform distribution of SiC particles in the composite. The SiC particles in the deposit have similar shape and size to those observed on the powder. The cross section of this composite coating also shows the uniform distribution of particles throughout the deposits, and it has a uniform thickness of about 34µm for 30 min of electrodeposition.

From these experiments, the following conclusion has been proposed:

Without much technical effort and even with the much lower particle concentration in the bath, AZTAB enhanced the codeposition of SiC particles in the Ni deposit up to an average of 62.4vol %. It is proposed that the differences in the desorption of surfactants from the particle surface due to their electrochemical reduction at the cathode surface are responsible for the effect of AZTAB and other surfactants on the extent of the codeposition of SiC particles. The particle loading, current density and the temperature of the bath were also found to have the significant influence on the extent of codeposition.

8) Ni-Diamond composite coatings- Effect of particle size on the content of Diamond in composite plating

Takebe et al.¹⁰⁾ studied the codeposition of Ni-Diamond composite coatings from Watts bath using the surfactant (AZTAB) to enhance the codeposition of Diamond into Ni matrix.

The content of the Diamond in Ni-Diamond composite coatings was found to have the maximum value of 46vol % which is much higher value usually obtained from the similar bath without surfactant.

In the wear properties of the composite coatings thus obtained, the wear loss of the coatings decreased with an increase of the content of Diamond in the deposit up to about 46%.

The content of Diamond in the composite coatings depends on the particle size of the Diamond as shown bellow:

Content of Diamond in the coatings.	
Particle size	Content of Diamond
2-3 µm	27 vol. %
1-2 µm	46 vol. %

9) Electrodeposition of Cu-graphite composite film from Copper sulfate bath

H. Hayashi¹¹⁾ studied the electrodeposition of Cu-graphite composite film from copper sulfate bath containing graphite particle. The role of the functional groups on the graphite edge during Cu-graphite composite plating was evaluated by the potentiometric titration method. He also carried out the deposition of Cu-graphite composite film by using a rotating disc electrode from

acid Cu sulfate bath in the presence of graphite particle. Upon analyzing the surface morphology of the Cu-graphite composite coating, it is found that the specific ordered structure of the coating can be fabricated by controlling the pH of the bath. In general, in the preparation of composite coating, the reaction seemed to occur in the vicinity of the working electrode. Therefore, these processes could be influenced by the chemical anisotropy (hydrophilic or hydrophobic) of the graphite particle. The functional groups, such as carboxyl- or phenolic hydroxide in the edge of the graphite particle, generally acts as an acid or a base when graphite is contact with the electrolyte. The evaluation of the acidity of the compounds has already been carried out by the ζ potential measurement and also by the mass titration method.

In this paper, potentiometric titration method was used to check the reaction mechanism between graphite particle and depositing Cu^{2+} ion in the plating bath. The following electrolyte was used for the potentiometric titration.

Electrolyte 0.5 M CuSO_4
 0.5 M K_2SO_4
 H_2SO_4 to pH = 2.0
 Graphite

Titration was carried out by 1 M KOH, 0.05 cm³/drop, 60 s. interval.

Table 5 shows the composition and plating conditions for the composite plating.

Table 5 Bath composition and operating conditions

Electrolyte : 0.5 M CuSO_4
 H_2SO_4 to control pH of the bath
 Graphite 50 g/dm³
 Cathode: Rotating Cu disk electrode (19.6mm²)
 Anode : Cu plate
 Temp.: Room temp.
 Current density: 30 mA/cm²
 RPM: 1500 rpm
 Plating time: 2 hrs.

Ultrasonic agitation was applied to keep the homogeneous dispersion of the graphite particle.

a) Potentiometric titration

Fig. 15 shows the potentiometric titration curves. Before the titration , pH of the K_2SO_4 solution containing graphite is slightly higher than that of the same K_2SO_4 solution without the graphite. These results imply that the functional groups of the graphite seemed to act as a base to increase the pH of the bath.

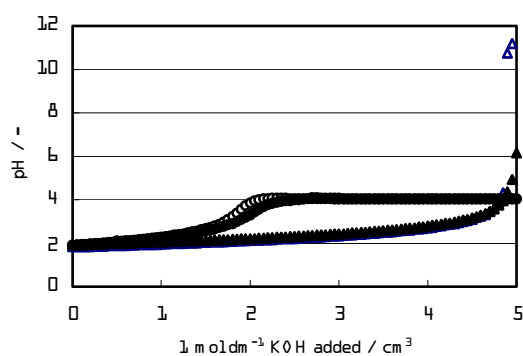


Fig. 15 Potentiometric titration curves of CuSO_4 and K_2SO_4 solution

- : 0.5 M K_2SO_4 50 cm^3 , ▲ : 0.5 M K_2SO_4 50 cm^3 + HAG150 2.5 g
 ○ : 0.5 M CuSO_4 50 cm^3 , ● : 0.5 M CuSO_4 50 cm^3 + HAG150 2.5 g

Based on the quantity of KOH used in this titration, it was found that the higher pH value was obtained up to 4.7 cm^3 of KOH. However, the both titration curves crossed each other at pH 3.7. Beyond this pH value, K_2SO_4 solution containing graphite gave rise to the lower pH value compared to the pure K_2SO_4 solution. These results also confirm the characteristics of the functional groups in the graphite acting as a base in this system. The pH of the crossing point of the both titration curves seemed to correspond to the pK_a of the compound which express the acidity of the functional group, probably carboxyl group in the edge of the graphite. The plateau region in the titration curves observed at around pH 4 indicated the formation of $\text{Cu}(\text{OH})_2$. Before the titration was started, CuSO_4 solution containing graphite particle gave the higher pH value compared to the same bath without graphite. Both titration curves crossed over each other at the pH 2.1 which is probably pK_a of the compound in the presence of Cu^{2+} in the bath. However, this value is found to be lower than the pH 3.7 in the same solution without Cu^{2+} ion. These results can be explained by the evolution of proton derived from the chemical reaction of Cu^{2+} with carboxyl group in graphite. This phenomena might be recognized by the adsorption of Cu^{2+} ion on the functional group of the graphite at the pH higher than the pK_a value.

b) Cu-graphite Composite plating

Judging from the potentiometric titration curves, the electrodeposition of Cu-graphite composite coating was carried out using a rotating disk electrode in 0.5 M CuSO_4 solution containing graphite particle.

Fig. 16 shows the SEM pictures of the electrodeposited Cu-graphite composite film in which co-deposition of graphite was observed at pH 2.03 and the surface morphology of the deposit seemed to be pure Cu deposit.

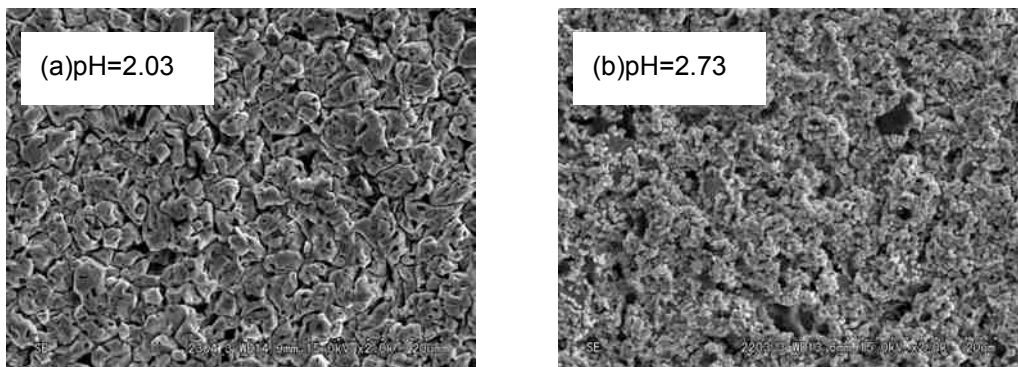


Fig. 16 SEM microphotographs of electrodeposits

(a) pH=2.03, 0.5 M CuSO₄, HAG150 50g/l (b) pH=2.73, 0.5 M CuSO₄, HAG150 50g/l

However, in the pH 2.73, the homogeneous co-deposition of graphite was observed in the Cu matrix. An increase in the pH of the plating bath resulted in the smooth co-deposition of graphite in the Cu matrix. This fact confirmed the adsorption of Cu²⁺ ion on the graphite surface.

Fig. 17 shows the surface morphology of the Cu-graphite composite coatings which indicate the initial state of the co-deposition.

The fine Cu crystal was observed around the edge of the graphite. These results suggest that the initial deposition seemed to occur at the edge of the graphite shown in the picture followed by extending the layer laterally to the basal plane which has the hydrophobic character. These results strongly reflect the chemical anisotropy of the graphite for the formation of composite coating.

Relationship between functional groups on the graphite and Cu²⁺ ion was confirmed to influence Cu-graphite composite plating by using the potentiometric titration method. Morphological aspect of the graphite particle revealed that the functional groups in the graphite seemed to be located at the edge of the graphite. Therefore, the Cu-graphite composite film which has the orientated structure might be fabricated by controlling pH of the bath and reaction conditions of the Cu²⁺ ion in the plating bath.

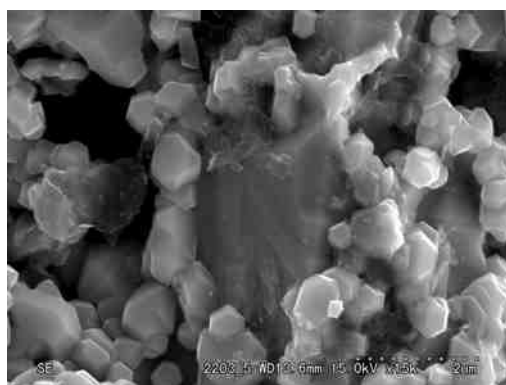


Fig. 17 SEM microphotograph of the electrodeposit from pH=2.73 solution 0.5 M CuSO₄, HAG150 50g/l

10) Ni composite coatings with hydroxide particles formed during electrolysis

Hayashi and Umemura¹²⁾ studied the Ni-Al hydroxide composite coatings from NiSO₄ + Al₂(SO₄)₃ bath. In general, pH of the vicinity of the cathode surface increases with the evolution of hydrogen in the Ni plating bath. In order to know much about the reaction mechanism of the Ni deposition, potentiometric titration of the 0.2 M NiSO₄ solution containing 0.01 M Al₂(SO₄)₃ was carried out by 1 M KOH solution.

Figure 18 shows the potentiometric titration curves.

Two plateau regions were observed in the titration curves. The former plateau was found at pH 4.2-4.7 and the latter at pH 7. The first plateau seemed to correspond to the formation of Al(OH)₃, and the latter to Ni(OH)₂.

From this picture, in the pH 4.5-5.5, Ni²⁺ does not seem to precipitate as a Ni(OH)₂, on the contrary, Al³⁺ ion tends to deposit as Al(OH)₃ in this pH region. Therefore, Al(OH)₃ might be co-deposited into Ni matrix when the electrolysis was carried out in this solution to give the nano-composite plating.

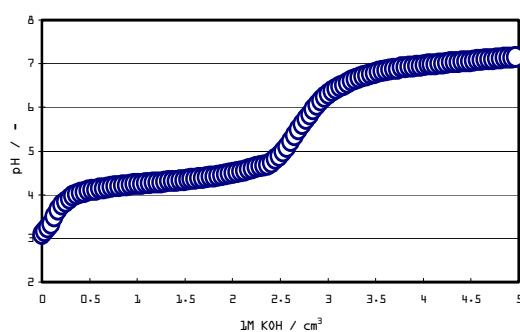


Fig. 18 Potentiometric titration curve of 0.2 M NiSO₄ + 0.01 M Al₂(SO₄)₃

The electrodeposition of Ni-Al oxide composite coating was shown in Table 6.

Table 6 Results of electrodeposition

	Bath A	Bath B
Al ³⁺	0.01 M	0.001 M
pH	3.70	3.85
Current efficiency	50~70%	□100%
Current density	20~100mA/cm ²	20~100mA/cm ²
Al/Ni(at%)	□55/45	Al□0
Temp.	45□	45□

Fig. 19 shows the SEM picture of the Ni composite coating obtained from the plating bath A at a current density of 50 mA/cm².

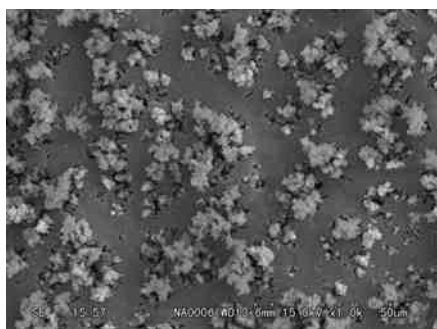


Fig. 19 SEM micrograph of Ni-Al(OH)₃
(Watts bath + Al₂(SO₄)₃, 50 mA/cm²)

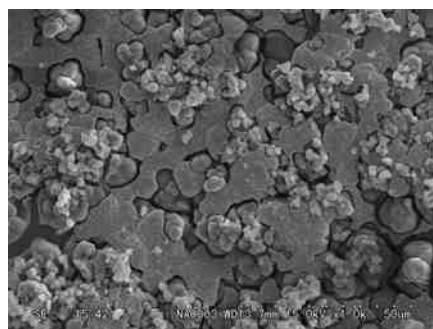


Fig. 20 SEM micrograph of Ni-Al(OH)₃
(Watts Ni bath + Al₂(SO₄)₃, 20 mA/cm²)

In this figure, agglomerated Al₂O₃ particles were found in the Ni matrix. When the electrolysis was carried out at 20 mA/cm², Al₂O₃ particles were homogeneously co-deposited in the Ni matrix as shown in Fig. 20.

When the very low concentration of Al³⁺ (0.001 M) was used, no co-deposition of Al(OH)₃ was observed in the Ni matrix owing to the slow change of the pH of the electrode surface due to the high current efficiency of the Ni deposition. Taking advantage of the increase in pH in the vicinity of the cathode surface, Ni composite coatings associated with hydroxide compounds might be prepared in the electrodeposition of Ni. Controlling the proper plating conditions to form hydroxide particles, the composite coatings with the highly ordered structure can be fabricated in the electrodeposition of Ni.

References

- 1) T. Hirato, J. of Surface Finishing Society Japan (S.F.S.J) **53**, 875 (2002)
- 2) J. Fransaer, E. Leunis, T. Hirato, J-P. Cellis, J. Applied Electrochem. **32**, 123 (2002)
- 3) T. Oda, A. Sato, T. Hirato, Y. Awakura, Paper #27-25 presented at the 107 meeting of S.F.S. J., March 25 (2003)
- 4) B. Ise, T. Sasaki, H. Katagiri, S. Meguro, J. of S.F.S.J. **51**, 1154 (2000)
- 5) F. Yamaguchi, T. Fujita, Y. Kanega, K. Ui, Y. Idemoto, N. Koura, Paper #18B-16 presented at the 108 meeting of S.F.S.J, Sep. 17 (2003)
- 6) T. Ibe, H. Kiyokawa, S. Yonezawa, M. Takashima, J. of S.F.S.J. **51**, 1239 (2000):
T. Ibe, H. Kiyokawa, Yong-Bo Chong, S. Yonezawa, M. Takashima, Materials Science Research International **4**, 148 (1999)
- 7) N. K. Shrestha, T. Saji, Paper #1M29 presented at the annual meeting of Electro-chemical. Soc. Japan (2003)
- 8) Y. Fujiwara, H. Enomoto, J. of S.F.S.J. **51**, 1069 (2000)
- 9) N. K. Shrestha, I. Miwa, T. Saji, J. Electrochem. Soc. **148** C106 (2001)
- 10) T. Takebe, N. K. Shrestha, T. Saji, Paper #1M32 presented at the Autumn meeting of the Electrochem. Soc. Japan (2003)
- 11) H. Hayashi, private communication. To be published in the J. S.F.S.J (2004)
- 12) H. Hayashi, H. Umemura, Paper #18B-14 presented at the 108 meeting of the S.F.S.J. Sep. (2003)